Available online at www.sciencedirect.com
ScienceDirect
Microporous and Mesoporous Materials 105 (2007) 124–131
MICROPOROUS AND MESOPOROUS MATERIALS
www.elsevier.com/locate/micromeso

Mixture diffusion in zeolites studied by MAS PFG NMR and molecular simulation

Moises Fernandez [a], Jörg Kärger [a], Dieter Freude [a,*], André Pampel [b], J.M. van Baten [c], R. Krishna [c]

[a] *Abteilung Grenzflächenphysik, Universität Leipzig, Linnéstraße 5, 04103 Leipzig, Germany*
[b] *Max Planck Institute for Human Cognitive and Brain Science, Stephanstraße 1a, 04103 Leipzig, Germany*
[c] *Van 't Hoff Institute for Molecular Sciences, University of Amsterdam, Nieuwe Achtergracht 166, 1018 WV Amsterdam, The Netherlands*

Received 18 December 2006; received in revised form 15 April 2007; accepted 23 May 2007
Available online 12 June 2007

Abstract

A combination of magic-angle spinning (MAS) and pulsed field gradient (PFG) NMR has been used to determine the self-diffusivities in MFI zeolite of *n*-butane, $D_{n\mathrm{C4}}$, in mixtures with *iso*-butane in which the total loading, q, is maintained constant at 4 molecules per unit cell. When the loading of *i*C4 in the mixture, $q_{i\mathrm{C4}}$, is increased from 0 to 2, the diffusivity $D_{n\mathrm{C4}}$ is observed to decrease dramatically by two orders of magnitude. Snapshots obtained from molecular simulations indicate that the *i*C4 molecules are preferentially located at the intersections between the straight channels and zig-zag channels of MFI; these intersections serve as traffic junctions. At $q_{i\mathrm{C4}} = 2$, the molecular traffic along the straight channels is brought to a virtual stand-still because of the obstructive influence of slow-diffusing *i*C4 ensconced at these junctions. Molecular dynamics (MD) simulations of $D_{n\mathrm{C4}}$ in *n*C4/*i*C4 mixtures show good qualitative agreement with the observed experimental results.

In sharp contrast, both experimental measurements and MD simulations, of $D_{n\mathrm{C4}}$ and $D_{i\mathrm{C4}}$ in wide pore FAU zeolite yield $D_{n\mathrm{C4}} \approx D_{i\mathrm{C4}}$ and there is no influence of mixture composition on component diffusion.

Keywords: Mixture diffusion; Zeolites; MFI; FAU; Butane isomers; Magic angle spinning; Pulse field gradient; Nuclear magnetic resonance; Molecular dynamics; Traffic junction effect

1. Introduction

NMR diffusiometry is a most powerful technique to investigate diffusion phenomena inside nanopores. It is able to follow molecular displacements from some hundreds of nanometers up to hundreds of micrometers. For diffusion within zeolites, NMR diffusiometry is able to provide direct information on both intra-crystalline diffusion and the so-called long-range diffusion, i.e. the rate of molecular propagation through beds of crystallites or in compacted particles [1]. However, there are difficulties associated with NMR measurements of mixture diffusion within zeolites. Firstly, the heterogeneities in the magnetic susceptibility of zeolite crystallites and the restricted molecular mobility in the zeolite framework cause a broadening of the NMR signal and make the resolution of the components in the mixture difficult. Secondly, the shorter relaxation times limit the duration of the gradient pulses. Thirdly, the reduced molecular mobility in zeolite crystallites leads to short diffusion paths during the observation time.

The combination of pulsed field gradient (PFG) NMR with magic-angle spinning (MAS) NMR has advantages in comparison with conventional PFG NMR, when applied to diffusion measurements in zeolites [2,3]. First, the increased resolution in the ppm scale allows us to monitor separately the different components of a mixture.

* Corresponding author. Tel.: +49 341 9732503; fax: +49 341 9739349.
E-mail address: freude@uni-leipzig.de (D. Freude).

1387-1811/$ - see front matter © 2007 Elsevier Inc. All rights reserved.
doi:10.1016/j.micromeso.2007.05.042

Notation

D	self-diffusivity ($m^2\ s^{-1}$)
$D_{n\mathrm{C4}}$	self-diffusivity of *n*C4 ($m^2\ s^{-1}$)
$D_{i\mathrm{C4}}$	self-diffusivity of *i*C4 ($m^2\ s^{-1}$)
g	field gradient ($T\ m^{-1}$)
p_π	duration of the π-pulse (s)
q	total mixture loading (molecules per unit cell)
$q_{i\mathrm{C4}}$	loading of *i*C4 in mixture (molecules per unit cell)
T	absolute temperature (K)

Greek letters

β	factor define by Eq. (1) (dimensionless)
γ	gyromagnetic ratio (dimensionless)
δ	gradient pulse width (s)
Δ	diffusion time (s)
τ	inter-gradient delay (s)

Second, the longer transverse relaxation time upon MAS allows more time for the application of magnetic field gradients and thus more sensitivity towards small molecular displacements.

The narrowing of signals achieved by MAS is demonstrated for a mixture of *n*-butane (*n*C4) and *iso*-butane (*i*C4) adsorbed in FAU zeolite (in the form of NaX, with Si/Al = 1.2) in Fig. 1. Without sample rotation, the spectrum consists of one broad peak with an full width at half maximum (fwhm) of 1275 Hz, without any possibility of differentiating between the two contributions. At a rotation frequency of 10 kHz, the spectra of *n*C4 and *i*C4 are well resolved in the peaks of the CH_2 and CH groups. Even the signal of the CH_3 groups shows a splitting of 0.1 ppm, the fwhm of the CH_3 signals is about 15 Hz.

The major objective of the current work is to investigate self-diffusion in *n*C4/*i*C4 mixtures in two types of zeolites FAU (wide pore) and MFI (medium pore) using MAS PFG NMR. We aim to demonstrate that the diffusion characteristics of these two zeolites are markedly different,

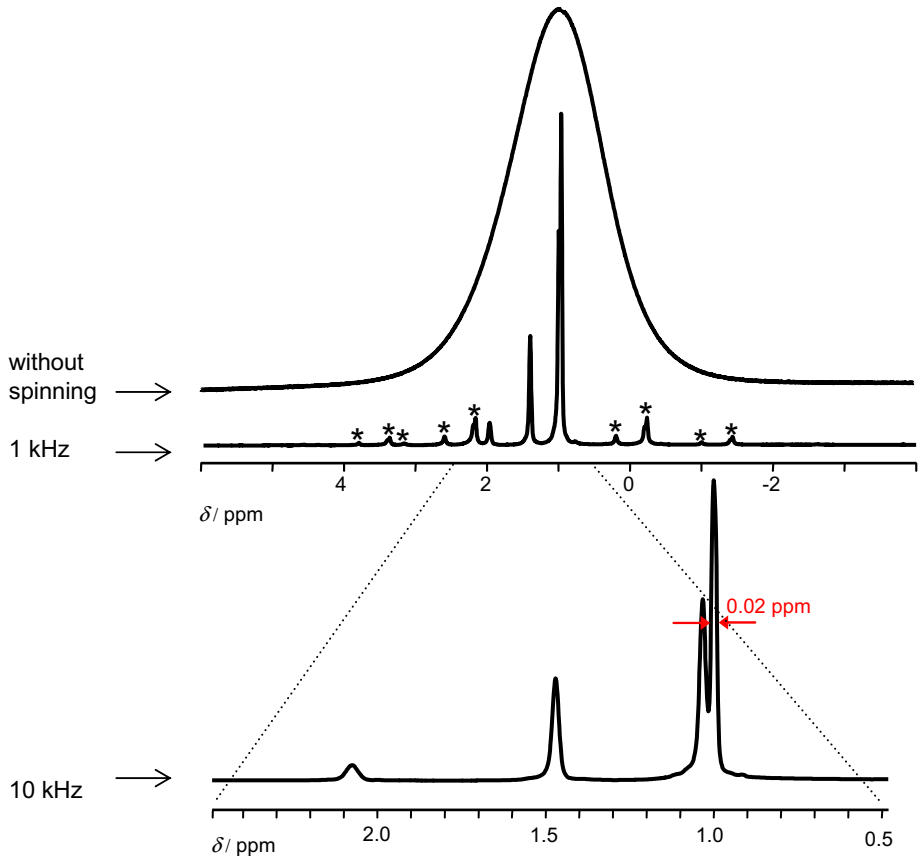

Fig. 1. ^{1}H MAS NMR spectra of an equimolar mixture of *n*C4 and *i*C4 adsorbed in FAU (NaX, with Si/Al = 1.2). Measurements were performed at 300 K, upper spectrum without sample spinning, middle spectrum with a MAS frequency of 1 kHz, lower spectrum with a MAS frequency of 10 kHz. Asterisks denote spinning side bands.

and that within the intersecting channels of MFI, the "traffic-junction" effect prevails. Molecular simulations are used to provide insights in the mixture diffusion characteristics.

2. Experimental procedure

MFI zeolite (in the all-silica form, silicalite-1) with a crystallite size in the range from 10 μm × 10 μm × 100 μm to 20 μm × 20 μm × 200 μm was kindly provided by Dr. Wolfgang Schmidt, MPI Mülheim. FAU zeolite (in the form NaX) was provided by Dr. Xiaobo Yang, University of Hannover. It has a crystallite size of about 50 μm and a Si/Al ratio of 1.2. The samples for the NMR measurements were prepared by heating 20 mg of the zeolite sample in glass tubes of 3 mm outer diameter. The temperature was increased under vacuum at a rate of 10 K h^{-1}. The samples were maintained at 673 K for 24 h under vacuum (less than 10^{-2} Pa). The zeolites were loaded with *n*C4 and *i*C4 at room temperature with a total loading, q, of 4 and 16 molecules per unit cell for the zeolites MFI and FAU, respectively. Then the glass tube (8 mm length) was sealed off.

NMR experiments were performed on a Bruker AVANCE spectrometer operating at 750 MHz with a wide-bore magnet. A Bruker 4 mm MAS probe with pulsed field gradient capabilities was used. The typical 90°-pulse-length was 10 μs. The maximum gradient strength in this system, $g_{max} = 0.54$ T m^{-1}. Diffusion measurements were performed using the stimulated-echo sequence with bipolar gradient pulses and eddy current delay before detection, see Fig. 2. The signal attenuation for single-component isotropic diffusion is given by

$$S = S_0 \exp\left[-D\left(\frac{4\delta g\gamma}{\pi}\right)^2\left(\Delta - \frac{\delta+\tau}{2} - \frac{\delta}{6} - p_\pi\right)\right] = S_0 \exp[-D\beta] \quad (1)$$

where D denotes the self-diffusion coefficient, γ the gyromagnetic ratio, δ the gradient pulse width, Δ the diffusion time, τ the inter-gradient delay, and p_π the duration of the π-pulse. The factor β is defined by Eq. (1). The delay between gradient pulse and subsequent r.f. pulse was 500 μs, in order to ensure that the duration of the dephasing and rephasing period is a multiple of the rotor period. Sinusoidal gradients with 2 ms duration were applied.

Diffusion experiments were carried out by varying the strength of gradient pulses between 10% and 90% of their maximum value that amounts to $g_{max} = 0.54$ T m^{-1}. We did not use the full gradient range for two reasons. First, linearity between the adjusted value and the gradient strength is only ensured between 4% and 90%. Second, for bipolar gradients and a 16-phase-cycle, in addition to the stimulated echo, the signal contains further contributions which are not averaged out by the phase cycle, but they disappear under the influence of the applied field gradients. Hence, experimental data for too small gradient intensities may assume values exceeding the actual ones and therefore have to be omitted. Therefore, the correct value of S_0 is not accessible by direct measurement. In case

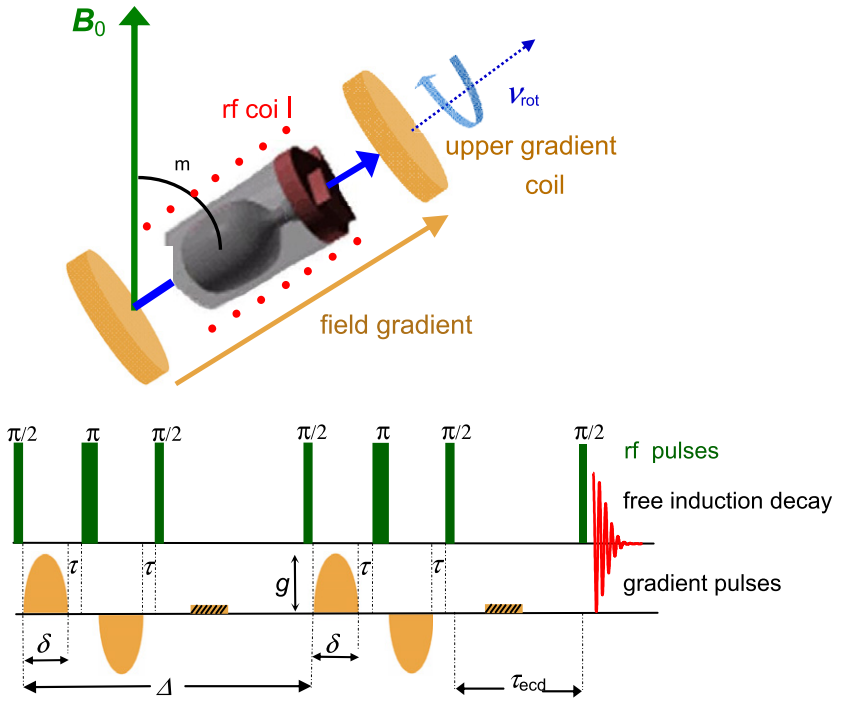

Fig. 2. A pictorial representation of the MAS design combined with anti-Helmholtz-coils for the pulsed field gradients in a high-resolution MAS NMR probe is shown at the top. The orientation of the spinning axis with respect to the external magnetic field is $\theta_m = \arccos 3^{-1/2} \approx 54.7°$. Radio frequency (r.f.) and gradient pulse scheme of the MAS PFG NMR experiment is shown below. The parameters are diffusion time Δ, gradient pulse width δ, gradient pulse strength g, eddy current delay τ_{ecd}, inter-gradient delay τ. Two weak rectangular shaped spoiler gradients average undesirable coherences.

of sufficient signal-to-noise ratio, the value S_0 has been estimated by extrapolating the first three experimental points (with gradient strengths above the 10% limit).

A short transverse relaxation time T_2 limits the duration of the gradient pulses and decreases the signal-to-noise ratio. MAS extends T_2 by a factor of 100 for FAU and we obtain $T_2 \approx 40$ ms, see line narrowing in Fig. 1. For *n*C4 and *i*C4 in MFI, at 363 K, values of T_2 under MAS conditions are about 5 ms and 3 ms, respectively. At 300 K, the T_2 of *i*C4 drops to 2 ms. However, as a consequence of the low diffusivity (and of the given upper value of the gradient intensity) gradient pulse durations that are two times larger are needed, so that a dramatic reduction of the MAS NMR signal even without the effect of the pulsed field gradient is inevitable. In order to reduce this effect, the number of accumulations is varied from 16 to 1024.

Eq. (1) is valid for isotropic one-component diffusion. For diffusion anisotropy the attenuation is more complicated. As an example, for two-dimensional diffusion [4] with $D_z = 0$ and $D_x = D_y = D_{2D} = (3/2)\ D_{eff}$, we have

$$S/S_0 = \exp[-D_{2D}\beta] \int_0^1 \exp[D_{2D}\beta t^2]\,dt \qquad (2)$$

One may define an effective diffusion coefficient in the case of anisotropic diffusion; see chapter 7.2 of Kärger and Ruthven [5]

$$D = (D_x + D_y + D_z)/3 \qquad (3)$$

which directly results from the first part of the echo attenuation, where it may be approached by a single exponential curve. As expected, there was no anisotropy effect of diffusion in FAU. By contrast, the well-known diffusion anisotropy in the MFI is known to cause a deviation from the single-exponential decay [6]. Under the given experimental conditions (low diffusivity, small signal intensities) it was impossible to use the experimental data for the determination of the principal elements D_x, D_y and D_z of the diffusion tensor, as it was realized for example in Hong et al. [6]. In such cases (notable deviations from a single-exponential behavior) we used only the first five points of our experimental curves for the determination of the effective diffusivity.

3. Experimental results for diffusion in FAU

Three samples of zeolite FAU were used with a total loading, q, of 16 molecules per unit cell; this amounts to 2 molecules per cavity of FAU. The first sample was loaded with *n*C4, the second with *i*C4, and the third with an equimolar mixture of *n*C4 and *i*C4. ^{1}H MAS NMR spectra are presented in Fig. 3a. A stack-plot of the ^{1}H MAS PFG NMR spectra of the *n*C4/*i*C4 equimolar mixture absorbed in FAU as function of the increasing pulsed gradient strength is presented in Fig. 3b. We used a diffusion time of $\Delta = 200$ ms and a gradient pulse length of $\delta = 0.5$ ms and performed the measurements at 300 K and at 363 K. Fig. 4 shows the decay of the CH_2 and CH signals of the

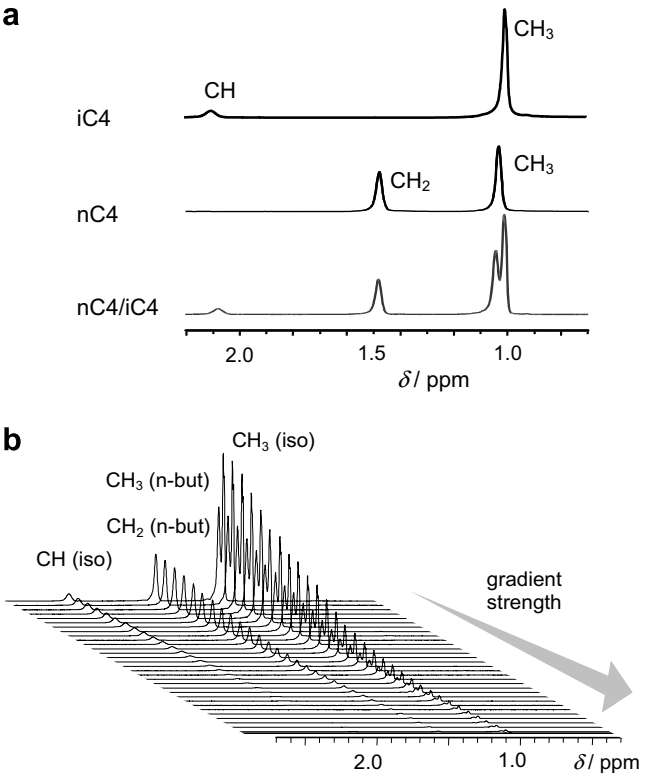

Fig. 3. (a) ^{1}H MAS NMR spectra of pure *n*C4, *i*C4 and *n*C4/*i*C4 mixture diffusion in FAU. The spectra refer to *i*C4 (top), *n*C4 (middle) and *n*C4/*i*C4 mixture (bottom). (b) Stack plot of the ^{1}H MAS PFG NMR spectra of the equimolar *n*C4/*i*C4 mixture absorbed in FAU as function of increasing pulsed gradient strength for a diffusion time $\Delta = 100$ ms. The total mixture loading, $q = 16$.

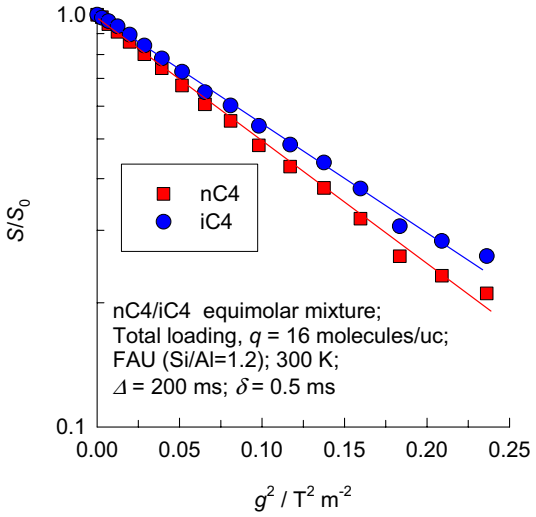

Fig. 4. Semi-logarithmic plot of the decay of the CH_2 and CH signals of the single components *n*C4 and *i*C4 in FAU (NaX, with Si/Al = 1.2) at 300 K. The diffusion time $\Delta = 200$ ms and a gradient pulse length $\delta = 0.5$ ms.

mixture. The values of the self diffusivities for pure *n*C4, *i*C4 and in *n*C4/*i*C4 mixtures at 300 K and 363 K are summarized in Figs. 5a and b. The values of D_{nC4} and D_{iC4}

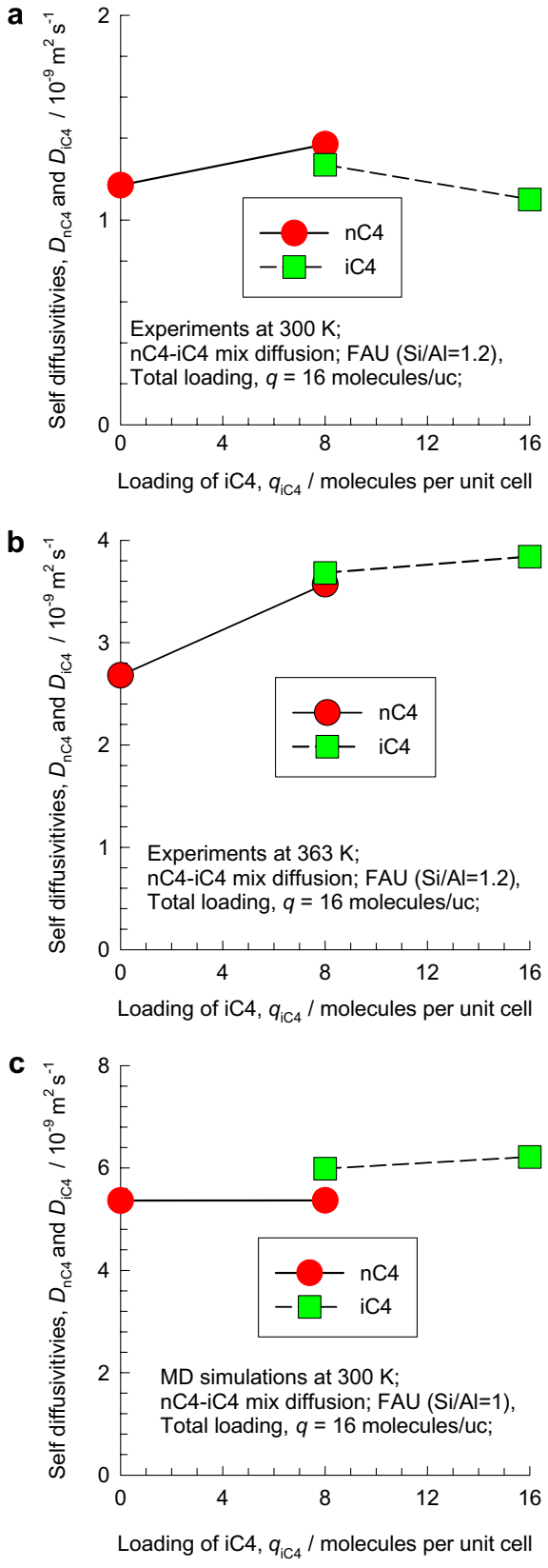

Fig. 5. Experimentally determined self diffusivities of *n*C4 and *i*C4, both for pure components and in equimolar mixture, in FAU (NaX, Si/Al = 1.2) at (a) 300 K and (b) 363 K. (c) MD simulations of self-diffusivities in FAU (Si/Al = 1) at 300 K. The total mixture loading, $q = 16$.

show no significant influence of the diffusion time. At 300 K we obtain for $\Delta = 20$ ms the value $D_{iC4} = 1.09 \times 10^{-9}$ m^2 s^{-1}, whereas for $\Delta = 200$ ms we have $D_{iC4} = 1.37 \times 10^{-9}$ m^2 s^{-1}. At 363 K we obtain for $\Delta = 50$ ms the value $D_{nC4} = 2.89 \times 10^{-9}$ m^2 s^{-1}, whereas for $\Delta = 200$ ms we get $D_{nC4} = 2.68 \times 10^{-9}$ m^2 s^{-1}. It should be noted that the accuracy of the experimentally determined self-diffusion coefficients can be given only within ±10% despite the fact that the error bar of individual points in graphs such as Fig. 4 is less than ±10%. It can therefore be concluded that the data on D is not influenced significantly by choice of the Δ.

Kärger et al. [7] obtained by PFG NMR in FAU (NaX) at $q_{nC4} = 8$, a value of $D_{nC4} = 1.3 \times 10^{-9}$ m^2 s^{-1} at 300 K. Our value of $D_{nC4} = 1.17 \times 10^{-9}$ m^2 s^{-1} at $q_{nC4} = 16$ is in reasonable agreement with their results.

It is interesting to note that both temperatures the D_{nC4} and D_{iC4} are nearly equal to one another in the mixture. At 363 K the measured data show D_{iC4} to have a slightly *higher* diffusivity than D_{nC4}. To rationalize these data, we performed MD simulations for diffusivities D_{nC4} and D_{iC4} in FAU (Si/Al = 1.0) at 300 K; the details of the MD simulation methodology are given in the Supplementary Material. The MD simulation results in Fig. 5c show that the diffusivities of either isomer are within ±10% of each other. It is also to be noted that the MD simulations predict a slightly higher diffusivity for the branched isomer, because the configuration of this molecule is more compact than that of *n*C4.

4. Experimental results for diffusion in MFI

Samples of MFI were used at a total loading, $q = 4$ molecules per unit cell. Pure *n*C4, and *i*C4, along with *n*C4/*i*C4 mixtures of varying compositions were used. ^{1}H MAS NMR spectra (not shown here) allow an examination of the loading of the mixtures by comparison of the CH and CH_2 peaks.

For diffusion of pure *i*C4, Fig. 6 shows the decays of the CH_3 signals at 300 K and 363 K. The self-diffusion coefficients measured for a diffusion time of $\Delta = 400$ ms are $D_{iC4} = 1.63 \times 10^{-12}$ m^2 s^{-1} and $D_{iC4} = 2.32 \times 10^{-12}$ m^2 s^{-1} for 300 K and 363 K, respectively. Additional measurements with $\Delta = 200$ ms at 363 K did not yield a significant difference in the value obtained with $\Delta = 400$ ms for D_{iC4}.

Banas et al. [8] were the first to determine D_{iC4} in MFI using PFG NMR. At 363 K, they report a value $D_{iC4} = 2 \times 10^{-12}$ m^2 s^{-1}, which was obtained, however, at a very poor signal-to-noise ratio. Millot et al. [9] used QENS to determine a value $D_{iC4} = 2.1 \times 10^{-12}$ m^2 s^{-1} at 398 K. Our value of 2.32×10^{-12} m^2 s^{-1}, at $q_{iC4} = 4$, is in reasonable agreement with their QENS data.

Also for *n*C4 a variation of the diffusion time Δ does not significantly affect the values of D_{nC4}; we obtained at 363 K values of $D_{nC4} = 6.42 \times 10^{-9}$ m^2 s^{-1} and 9.87×10^{-9} m^2 s^{-1} for $\Delta = 20$ and 200 ms, respectively. At 300 K, the value of $D_{nC4} = 3.55 \times 10^{-1}$ m^2 s^{-1} was obtained with $\Delta = 30$ ms.

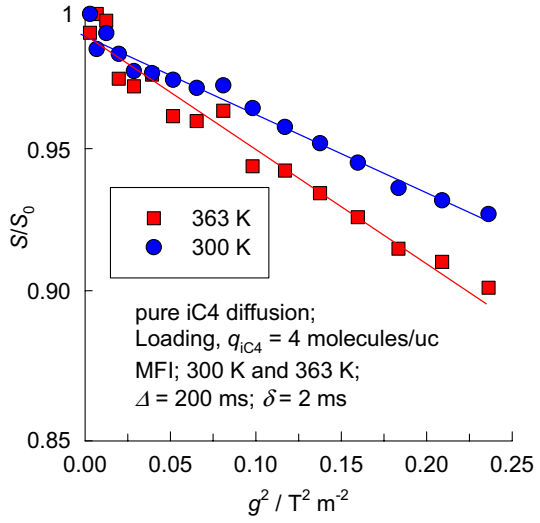

Fig. 6. Semi-logarithmic plot of the signal attenuation of the signal attenuation of the CH_3 group of *i*C4 adsorbed in MFI at $T = 300$ K and 363 K. The diffusion time is $\Delta = 400$ ms and gradient pulse length is $\delta = 2$ ms.

Pampel et al. [2] measured by MAS PFG NMR at 300 K the value of $D_{n\mathrm{C4}} = 3.17 \times 10^{-1}\ \mathrm{m^2\ s^{-1}}$, in reasonable agreement with our results.

Heink et al. [10] obtained by PFG NMR at 290 K the value of $D_{n\mathrm{C4}} = 5.7 \times 10^{-1}\ \mathrm{m^2\ s^{-1}}$ for MFI. Values which are lower up to two orders of magnitude were obtained by other techniques, see Nijhuis et al. [11]. Banas et al. [8] found also by PFG NMR at 303 K a significant lower value of $D_{n\mathrm{C4}} = 1.4 \times 10^{-11}\ \mathrm{m^2\ s^{-1}}$.

Self diffusivities of *n*C4 were determined in *n*C4/*i*C4 mixtures with varying proportions of *n*C4 and *i*C4, keeping the total loading constant at $q = 4$. For the higher diffusivities in the mixtures we used smaller values of Δ. Higher diffusivities are obtained when the loading of *i*C4 in the mixture, $q_{i\mathrm{C4}} < 2.5$; for these cases, $\Delta = 20$ ms. Significantly lower diffusivities were obtained for $q_{i\mathrm{C4}} > 2.5$; for these cases $\Delta = 200$ ms was used. Pure *i*C4 was measured at $\Delta = 400$ ms.

In contrast to measurements in FAU, signal broadening in MFI inhibits resolution of the two CH_3 signals in the mixture. The intensity of the CH-signal is very low and could not be used for the determination of $D_{i\mathrm{C4}}$ in the *n*C4/*i*C4 mixture. Therefore, in mixtures we measured the attenuation of the CH_2-signal of *n*C4 molecules, see Fig. 7. The $D_{n\mathrm{C4}}$ are obtained by linear regression of the experimental data. Due to the diffusion anisotropy, the decay is not linear; the extent of non-linearity increases when $q_{i\mathrm{C4}} < 2.5$; see Fig. 7. In order to determine the $D_{n\mathrm{C4}}$ in the mixtures we consider the initial portion of the decay curve and the first five experimental points; this gives the *effective* value of $D_{n\mathrm{C4}}$, see Eq. (3). Fig. 8 presents a semi-log plot of $D_{n\mathrm{C4}}$ in the mixture as a function of $q_{i\mathrm{C4}}$; also included in this figure is the data for $D_{i\mathrm{C4}}$ at $q_{i\mathrm{C4}} = 4$. The data is remarkable because we notice that $D_{n\mathrm{C4}}$ reduces by two orders of magnitude when $q_{i\mathrm{C4}}$ is increased from 0 to 2. This dramatic reduction is best appreciated by plotting the same data on linear axes, as shown in Fig. 8b. We note that the $D_{n\mathrm{C4}}$ reduces to near-zero values in a *linear* fashion as the loading $q_{i\mathrm{C4}}$ is increased from 0 to 2. In order to understand and explain the reason for the reduction of $D_{n\mathrm{C4}}$ to near-zero values at $q_{i\mathrm{C4}} = 2$, we resort to molecular simulations.

5. Molecular simulations

We performed two types of simulations. Firstly, Configurational-Bias Monte Carlo (CBMC) simulations were performed in order to determine the equilibrium spatial distribution of *n*C4 and *i*C4 within the channels of MFI zeolite. Secondly, molecular dynamics (MD) simulations

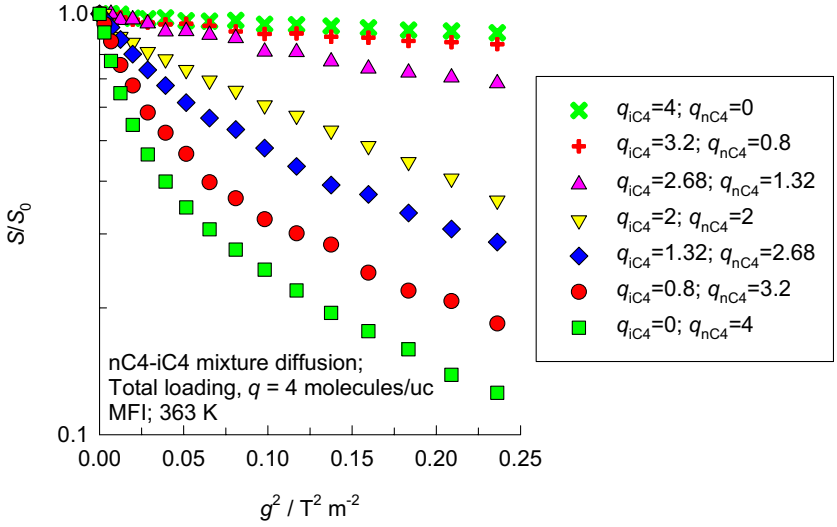

Fig. 7. Attenuation of the CH_2 signals of *n*C4 in pure *n*C4 and in *n*C4/*i*C4 mixtures and of the CH_3 signal of pure *i*C4 in MFI at $T = 363$ K. In all samples, the total mixture loading $q = 4$.

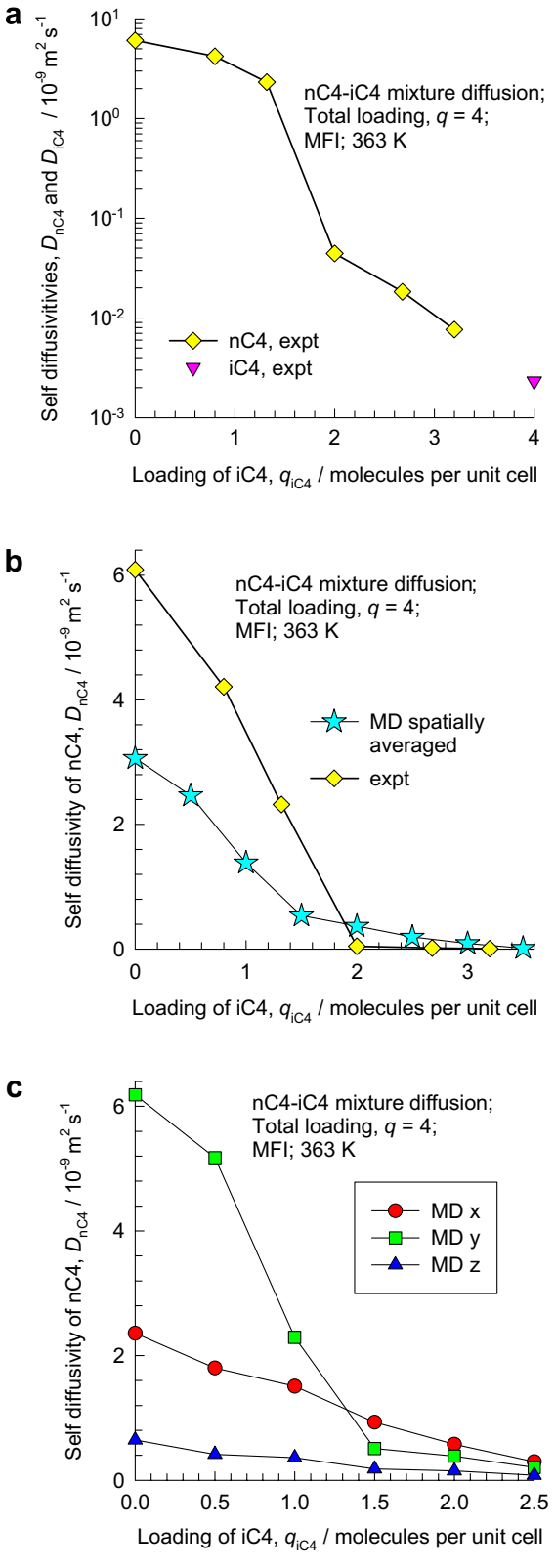

Fig. 8. (a) Experimental data on self-diffusion coefficients of *n*C4 in *n*C4/*i*C4 mixtures in MFI at 363 K as a function of the loading of *i*C4 in the mixture. Also shown is the self-diffusivity of pure *i*C4. (b) Spatially averaged value of D_{nC4} from MD simulations compared with experimental data for D_{nC4}. (c) MD simulations of the D_{nC4} in *n*C4/*i*C4 mixtures in MFI at 363 K in *x*-, *y*- and *z*-directions as a function of the loading of *i*C4 in the mixture. The total mixture loading, $q = 4$ in all cases.

were performed to determine D_{nC4} in *n*C4/*i*C4 mixture with varying composition keeping a total loading, $q = 4$. The CBMC and MD simulation methodologies are described in the Supplementary Material accompanying this publication; this also contains a variety of snapshots and detailed simulation results. A selection of these results is discussed below.

CBMC simulations show that whereas *n*C4 can locate along either straight or zig-zag channels of MFI, *i*C4 locates preferentially at the intersections because of configurational considerations [12]. The intersections provide more "leg-room" for *i*C4 molecules to locate; the branched isomer finds it difficult to locate within either the straight or zig-zag channels. For an equimolar mixture with a total

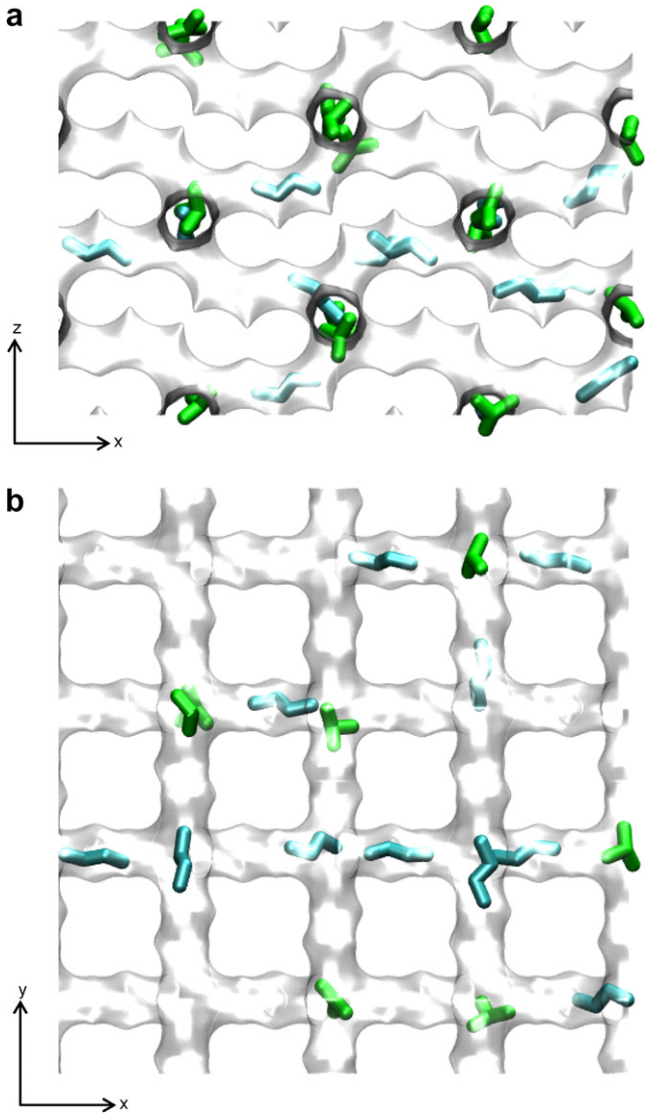

Fig. 9. Snapshots showing the location of *n*C4 (blue) and *i*C4 (green) molecules in silicalite-1, viewed (a) from the top, in the *x*–*z* plane, and (b) from the side, in the *x*–*y* plane. The total loading in this simulation snapshot is 4 molecules per unit cell, with equal amounts of each isomer. The side view is one unit cell deep. The top view is two unit cells deep. (For interpretation of the references to colour in this figure legend, the reader is referred to the web version of this article.)

loading, $q = 4$, Fig. 9 shows snapshots, viewed from (a) the top, and (b) along the sides. At the chosen component loadings, $q_{n\mathrm{C4}} = q_{i\mathrm{C4}} = 2$, only half the total number of intersections are occupied by *i*C4. Since the occupancy of the intersections is distributed randomly, each one of the straight channels has an *i*C4 molecule ensconced somewhere along the *y*-direction; this is evident from Fig. 9a, a view that is 2 unit cells deep, showing all intersections have at least one *i*C4 molecule. Our experimental data, presented in Fig. 8a, shows that the pure component $D_{i\mathrm{C4}}$ is about three orders of magnitude lower than $D_{n\mathrm{C4}}$. Consequently, the occupation of *i*C4 at the intersections of the channels is tantamount to blockage, leading to severe reduction in the molecular traffic of the more mobile *n*C4 along the straight channels in the *y*-direction.

For quantification of the traffic junction effect we performed MD simulations of the $D_{n\mathrm{C4}}$ various mixture compositions. Fig. 8c shows the MD simulation results for $D_{n\mathrm{C4}}$ in *x*-, *y*- and *z*-directions as function of *i*C4 loading, $q_{i\mathrm{C4}}$. Diffusion along the straight channels is the main contributor to diffusion and the increasing occupation of intersection sites by *i*C4 has a significant negative effect on the diffusivity. We see that $D_{n\mathrm{C4},y}$ is reduced to practically zero as $q_{i\mathrm{C4}}$ is increased from 0 to 2. It is also interesting to note that for $q_{i\mathrm{C4}} > 1.5$, $D_{n\mathrm{C4},y} < D_{n\mathrm{C4},x}$, suggesting that *n*C4 has to worm its way along the zig-zag channels because the traffic in the *y*-direction is at a practical stand-still at $q_{i\mathrm{C4}} = 2$. The spatially averaged $D_{n\mathrm{C4}} = (D_{n\mathrm{C4},x} + D_{n\mathrm{C4},y} + D_{n\mathrm{C4},x})/3$ is compared in Fig. 8b with the experimental value; both sets of results show a linear decline in $D_{n\mathrm{C4}}$ with increasing $q_{i\mathrm{C4}}$. The MD simulated $D_{n\mathrm{C4}}$ is about half of the experimental value; such a deviation is not uncommon [13] and is due to the extreme sensitivity of the MD simulations to the choice of the force fields.

6. Conclusions

Magic-angle spinning and pulsed field gradient NMR have been combined to study the intra-crystalline self-diffusion of *n*C4/*i*C4 mixtures in MFI and FAU. Using the MAS PFG combination the detrimental line broadening due to inevitable susceptibility heterogeneities in MFI which so far has prohibited highly resolved measurements has been dramatically reduced. This enabled selective diffusion measurements of species with chemical shift differences of less than 0.1 ppm.

Experimental measurements of $D_{n\mathrm{C4}}$ and $D_{i\mathrm{C4}}$ in wide pore FAU zeolite show $D_{n\mathrm{C4}} \approx D_{i\mathrm{C4}}$ and there is no influence of mixture composition on component diffusion. These results are in agreement with MD simulations.

In MFI, it was found that $D_{n\mathrm{C4}}$ in the mixture decreases with increasing loading of *i*C4. As $q_{i\mathrm{C4}}$ increases to a value of 2 molecules per unit cell, the $D_{n\mathrm{C4}}$ reduces by about two orders of magnitude. Molecular simulations have shown that at $q_{i\mathrm{C4}} = 2$, the molecular traffic of *n*C4 is brought to a virtual stand-still because of blocking of the intersection sites by *i*C4 molecules.

Acknowledgments

This work was supported by the Deutsche Forschungsgemeinschaft under the projects Pa 907/3-1 and GRK 1056/1 (International Research Training Group "Diffusion in Porous Materials") and by the Max-Buchner-Stiftung. RK acknowledges the grant of a TOP subsidy from the Netherlands Foundation for Fundamental Research (NWO-CW) for intensification of reactors and NWO/NCF for provision of high performance computing resources.

Appendix A. Supplementary data

Appendix A gives details of the CBMC and MD simulation methodologies. Snapshots showing location of the molecules in MFI and FAU, along with detailed simulation results are also included. Supplementary data associated with this article can be found, in the online version, at doi:10.1016/j.micromeso.2007.05.042.

References

[1] J. Kärger, S. Vasenkov, Micropor. Mesopor. Mater. 85 (2005) 195–206.
[2] A. Pampel, M. Fernandez, D. Freude, J. Kärger, Chem. Phys. Lett. 407 (2005) 53–57.
[3] A. Pampel, F. Engelke, P. Galvosas, C. Krause, F. Stallmach, D. Michel, J. Kärger, Micropor. Mesopor. Mater. 90 (2006) 271–277.
[4] B. Zibrowius, J. Caro, J. Kärger, Z. Phys. Chem. – Leipzig 269 (1988) 1101–1106.
[5] J. Kärger, D.M. Ruthven, Diffusion in Zeolites and Other Microporous Solids, Wiley & Sons, New York, 1992.
[6] U. Hong, J. Kärger, H. Pfeifer, U. Müller, K.K. Unger, Z. Phys. Chem. 173 (1991) 225–234.
[7] J. Kärger, H. Pfeifer, M. Rauscher, A. Walter, J. Chem. Soc., Faraday Trans. 76 (1980) 717–737.
[8] K. Banas, F. Brandani, D.M. Ruthven, F. Stallmach, J. Karger, Magn. Reson. Imaging 23 (2005) 227–232.
[9] B. Millot, A. Methivier, H. Jobic, H. Moueddeb, M. Bee, J. Phys. Chem. B 103 (1999) 1096–1101.
[10] W. Heink, J. Kärger, H. Pfeifer, K.P. Datema, A.K. Nowak, J. Chem. Soc., Faraday Trans. 88 (1992) 3505–3509.
[11] T.A. Nijhuis, L.J.P. van den Broeke, M.J.G. Linders, J.M. van de Graaf, F. Kapteijn, M. Makkee, J.A. Moulijn, Chem. Eng. Sci. 54 (1999) 4423–4436.
[12] T.J.H. Vlugt, W. Zhu, F. Kapteijn, J.A. Moulijn, B. Smit, R. Krishna, J. Am. Chem. Soc. 120 (1998) 5599–5600.
[13] H. Jobic, C. Laloué, C. Laroche, J.M. van Baten, R. Krishna, J. Phys. Chem. B 110 (2006) 2195–2201.

Supplementary Material to accompany

Mixture diffusion in zeolites studied by MAS PFG NMR and molecular simulation

Moises Fernandez[(1)], Jörg Kärger[(1)], Dieter Freude[(1)]*, André Pampel[(2)], J.M. van Baten[(3)] and R. Krishna[(3)]

[(1)] Abteilung Grenzflächenphysik, Universität Leipzig, Linnéstraße 5, 04103 Leipzig, Germany

[(2)] Max Planck Institute for Human Cognitive and Brain Science, Stephanstraße 1a, 04103 Leipzig, German

[(3)]Van 't Hoff Institute for Molecular Sciences, University of Amsterdam, Nieuwe Achtergracht 166, 1018 WV Amsterdam, The Netherlands.

* Corresponding author. Tel. +49 341 9732503; fax +49 341 9739349

E-mail address: freude@uni-leipzig.de

Appendix A: Molecular simulations methodology and results

1. CBMC simulations methodology

CBMC simulations have been carried out to determine the adsorption isotherms for nC4 and iC4 alkanes in MFI (all silica silicalite-1) at 363 K and for FAU (96 Si, 96 Al) at 300 K; the crystallographic data are available elsewhere[1, 2]. We use the united atom model. The zeolite framework is considered to be rigid. We consider the CH_x groups as single, chargeless interaction centers with their own effective potentials. The beads in the chain are connected by harmonic bonding potentials. A harmonic cosine bending potential models the bond bending between three neighboring beads, a Ryckaert-Bellemans potential controls the torsion angle. The beads in a chain separated by more than three bonds interact with each other through a Lennard-Jones potential. The Lennard-Jones potentials are shifted and cut at 12 Å. The CBMC simulation details, along with the force fields have been given in detail in earlier publications[3, 4]. The simulation box consists of 2×2×4 unit cells for MFI and 1×1×1 unit cell for FAU. Periodic boundary conditions were employed. It was verified that the size of the simulation box was large enough to yield reliable data on adsorption.

The CBMC simulations were performed using the BIGMAC code developed by T.J.H. Vlugt[5] as basis. The code was modified to handle rigid molecular structures and charges. S. Calero is gratefully acknowledged for her technical inputs in this regard.

2. MD Simulations methodology

Diffusion in a system of N molecules is simulated using Newton's equations of motion until the system properties, on average, no longer change in time. The Verlet algorithm is used for time integration. The energy drift of the entire system is monitored to ensure that the time steps taken were not too large. A time step of 1 fs was used in all simulations. N molecules are inserted into the framework at random positions as long as no overlaps occur with the framework or other particles, and as long as the positions are accessible from the main cages and channels. During the initializing period we perform an NVT MC simulation to rapidly achieve an equilibrium molecular arrangement. After the initialization step, we assign velocities to the pseudo-atoms from the Maxwell-Boltzmann distribution at the desired average temperature. The total momentum of the system is set to zero. Next, we equilibrate the system further by performing an NVT MD simulation using the Nosé-Hoover thermostat. When the equilibration is completed, the production run starts. For every cycle, the statistics for determining the mean square displacements (MSDs) are updated. The MSDs are determined for time intervals ranging from 2 fs to 1 ns. In order to do this, an order-N algorithm, as detailed in Frenkel and Smit[6] is implemented. The details on how diffusivities are determined from the MSDs are also to be found in Frenkel and Smit[6] and elsewhere.[2, 7] The Nosé-Hoover thermostat is used to main constant temperature conditions. The DLPOLY code[8] was used along with the force field implementation as described in the previous section. DL_POLY is a molecular dynamics simulation package written by W. Smith, T.R. Forester and I.T. Todorov and has been obtained from CCLRCs Daresbury Laboratory via the website[8].

The self-diffusivity, D_i, of component i in a mixture was computed by analyzing the MSDs of each component using

$$D_i = \frac{1}{2}\lim_{\Delta t\to\infty}\frac{1}{\Delta t}\left(\frac{1}{N_i}\sum_{l=1}^{N_i}\left(\mathbf{r}_{l,i}(t+\Delta t)-\mathbf{r}_{l,i}(t)\right)^2\right) \qquad (1)$$

for each of the three coordinate directions, x, y, and z. In Eq. (1) N_i represents the number of molecules of species i, and $\mathbf{r}_{l,i}(t)$ is the position at any time t.

For any specified loading three independent MD simulations (each running for 120 h on PCs equipped with Intel Xeon processors running at 3.4 GHz on the Linux operating system) were carried out to obtain good estimates of diffusivities and standard deviations of the results.

3. Simulation results

The CBMC simulations of the adsorption isotherms for pure nC4, and pure iC4 in MFI at 363 K are presented in Figure 1. Snapshots showing the location of the nC4 and iC4 molecules at different component loadings in the mixture are shown in Figures 2, 3, and 4. Note that the view in these snapshots are 2 unit cells deep. The pure component self-diffusivity of nC4 in MFI at 363 K is shown in Figure 5 as a function of total loading. The self-diffusivities are shown in x, y, and z directions, along with the spatially averaged values. The data for a loading of 4 molecules per unit cell is used for comparison with MAS PFG NMR experimental data. The self-diffusivity of nC4 in nC4/iC4 mixtures is shown in Figure 6. The self-diffusivities are shown in x, y, and z directions, along with the spatially averaged values. For iC4 loadings in the mixture higher than 2.5 molecules per unit cell, the nC4 self diffusivity values are too low to be accurately determined from MD simulations. It is remarkable to note that for iC4 loadings higher than 1.5 molecules per unit cell the D_y values are lower than the D_x values.

The pure component adsorption isotherms for nC4 and iC4 in FAU (Si/Al=1) at 300 K are shown in Figure 7. The self-diffusivities of the pure components and in an equimolar mixture are shown in Figure 8. The spatially average diffusivities are reported in Figures 7 and 8. It is remarkable to note that in contrast to the results for MFI (Figure 6), for FAU the diffusivities of nC4 and iC4 are nearly the same. This is in agreement with the MAS PFG NMR experimental data.

4. References

[1] C. Baerlocher, L.B. McCusker, Database of Zeolite Structures, International Zeolite Association, http://www.iza-structure.org/databases/, 26 June 2001.

[2] J.M. van Baten, R. Krishna, MD Simulations of Diffusion in Zeolites, University of Amsterdam, http://www.science.uva.nl/research/cr/md/,

[3] T.J.H. Vlugt, R. Krishna, B. Smit, Molecular simulations of adsorption isotherms for linear and branched alkanes and their mixtures in silicalite, J. Phys. Chem. B 103 (1999) 1102-1118.

[4] D. Dubbeldam, S. Calero, T.J.H. Vlugt, R. Krishna, T.L.M. Maesen, B. Smit, United Atom Forcefield for Alkanes in Nanoporous Materials, J. Phys. Chem. B 108 (2004) 12301-12313.

[5] T.J.H. Vlugt, BIGMAC, University of Amsterdam, http://molsim.chem.uva.nl/bigmac/, 1 November 2000.

[6] D. Frenkel, B. Smit, Understanding molecular simulations: from algorithms to applications, Academic Press, 2nd Edition, San Diego, 2002.

[7] R. Krishna, J.M. van Baten, Diffusion of alkane mixtures in zeolites. Validating the Maxwell-Stefan formulation using MD simulations, J. Phys. Chem. B 109 (2005) 6386-6396.

[8] W. Smith, T.R. Forester, I.T. Todorov, The DL_POLY Molecular Simulation Package, Warrington, England, http://www.cse.clrc.ac.uk/msi/software/DL_POLY/index.shtml, March 2006.

5. Captions for Figures

Figure 1. Pure component adsorption isotherms for nC4 and iC4 in MFI at 363 K obtained from CBMC simulations.

Figure 2. Snapshots showing location of nC4 and iC4 at mixture loadings (in molecules per unit cell) of (a) nC4 = 4, iC4 = 0, (b) nC4 = 3.5, iC4 = 0.5, and (c) nC4 = 3, iC4 = 1.

Figure 3. Snapshots showing location of nC4 and iC4 at mixture loadings (in molecules per unit cell) of (a) nC4 = 2.5, iC4 = 1.5, (b) nC4 = 2, iC4 = 2, and (c) nC4 = 1.5, iC4 = 2.5.

Figure 4. Snapshots showing location of nC4 and iC4 at mixture loadings (in molecules per unit cell) of (a) nC4 = 1, iC4 = 3, (b) nC4 =0.5, iC4 = 3.5, and (c) nC4 = 0, iC4 = 4.

Figure 5. MD simulations of pure component diffusion of nC4 at 363 K in MFI.

Figure 6. MD simulation results of self diffusivity of nC4 in nC4-iC4 mixtures at 363 K in MFI. The total loading is maintained at 4 molecules per unit cell.

Figure 7. Pure component adsorption isotherms for nC4 and iC4 in FAU (96 Si, 96 Al) at 300 K.

Figure 8. (a) Self diffusion of pure nC4 and iC4 in FAU (96 Si, 96 Al) at 300 K for various loadings. (b) Self diffusivities of nC4 and iC4 in equimolar nC4-iC4 mixtures at various loadings.

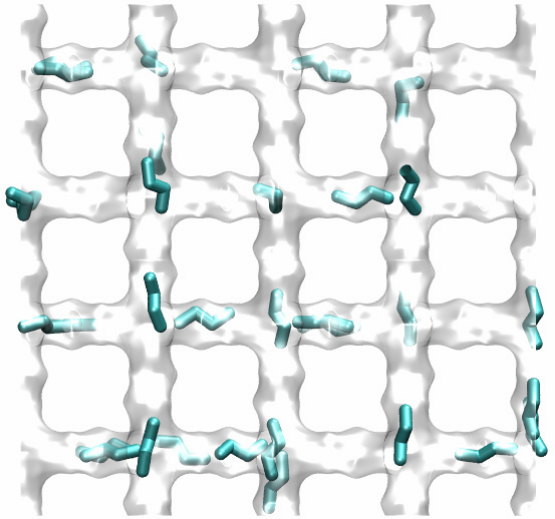

nC4 adsorbs along straight and zig-zag channels

the snapshots are 2 ucs deep

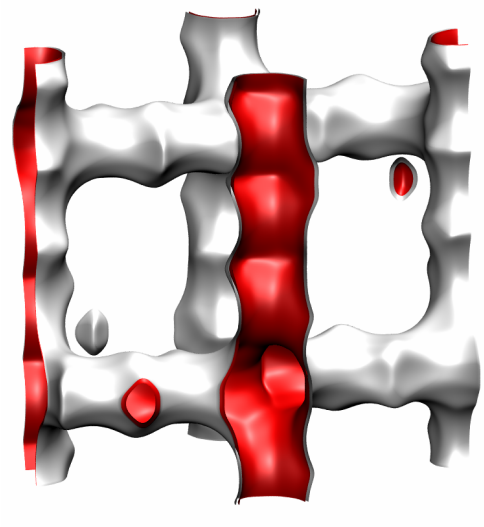

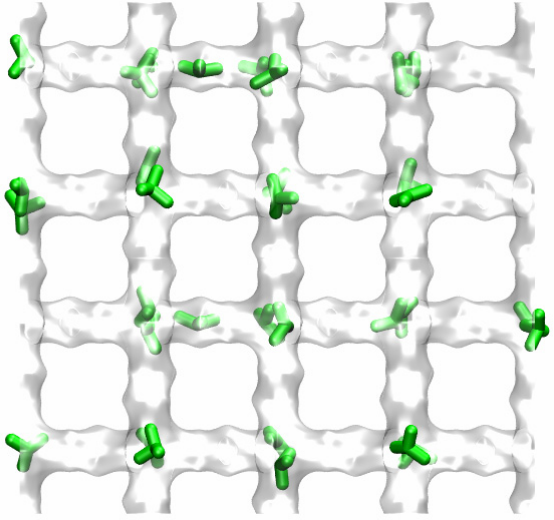

iC4 locates mainly at the intersections

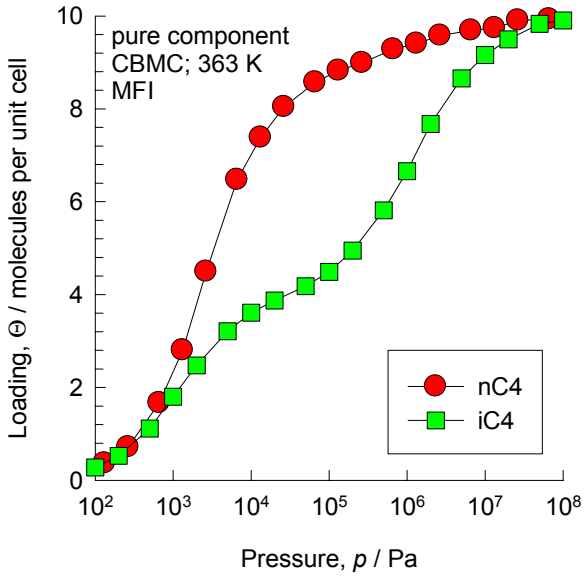

Pure component adsorption isotherms for nC4 and iC4 at 363 K in MFI

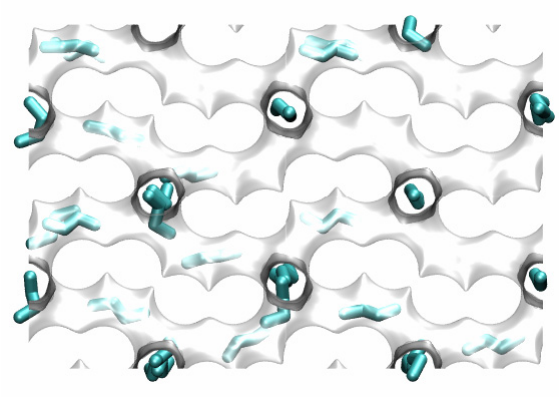

nC4 = 4 molecules/uc

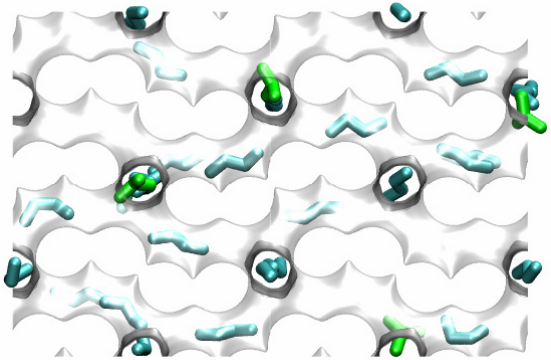

nC4 = 3.5 molecules/uc
iC4 = 0.5 molecules/uc

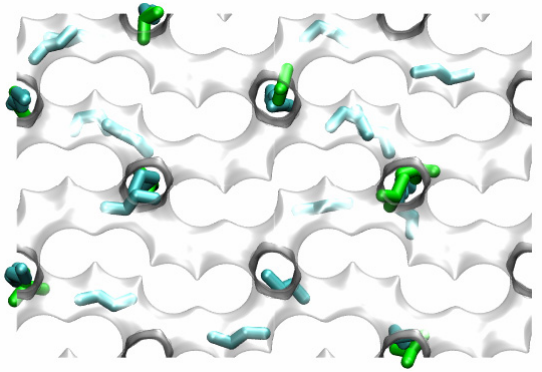

nC4 = 3 molecules/uc
iC4 = 1 molecules/uc

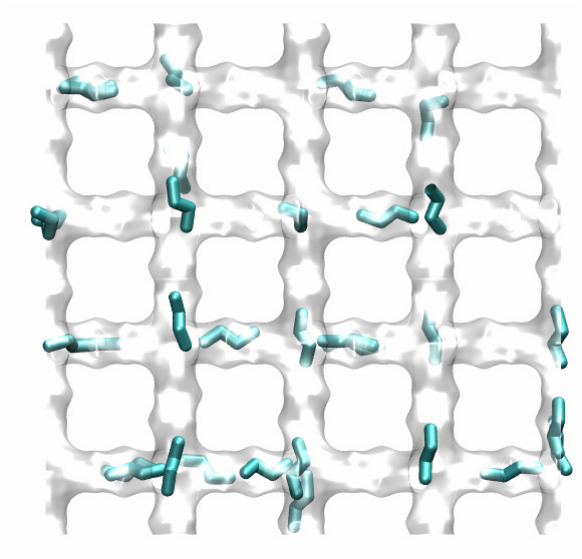

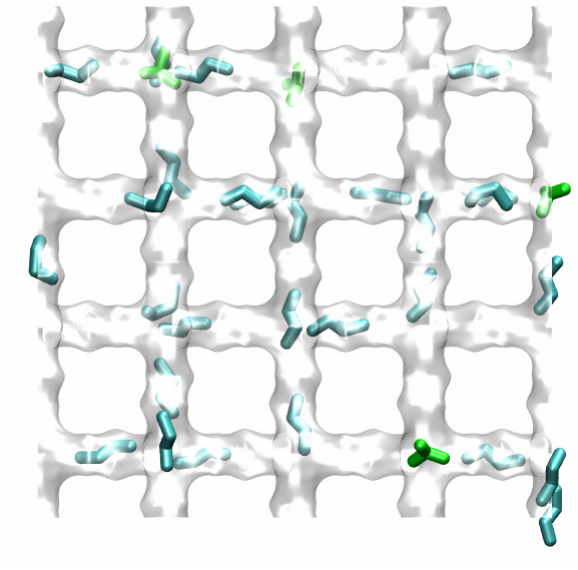

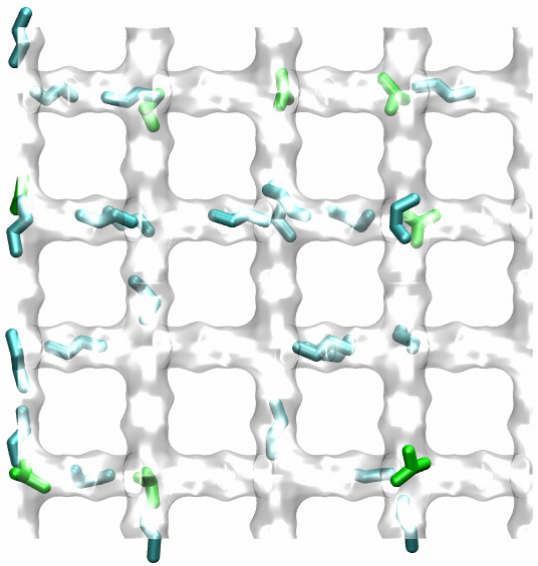

Snapshots showing location of nC4 - iC4 mixtures at in MFI at various loadings

the snapshots are 2 ucs deep

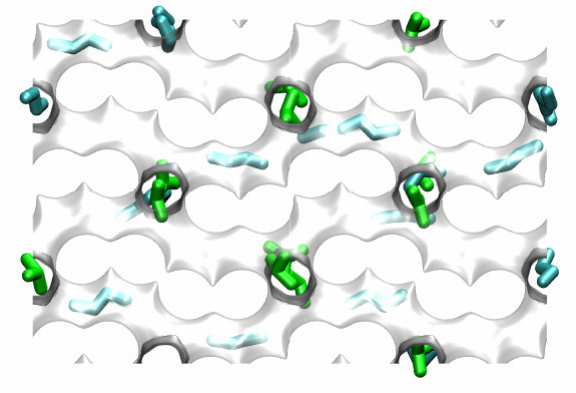

nC4 = 2.5 molecules/uc
iC4 = 1.5 molecules/uc

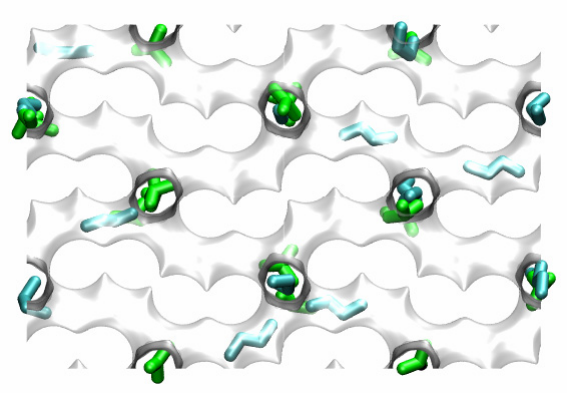

nC4 = 2 molecules/uc
iC4 = 2 molecules/uc

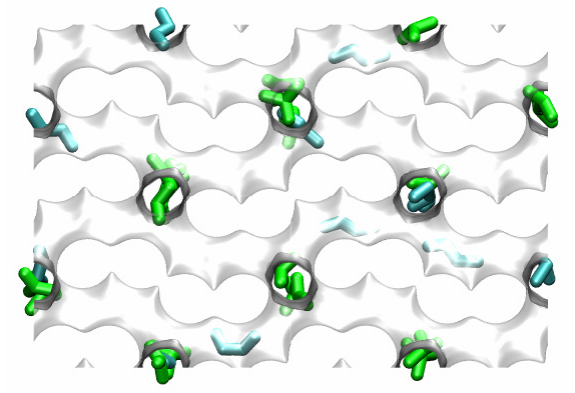

nC4 = 1.5 molecules/uc
iC4 = 2.5 molecules/uc

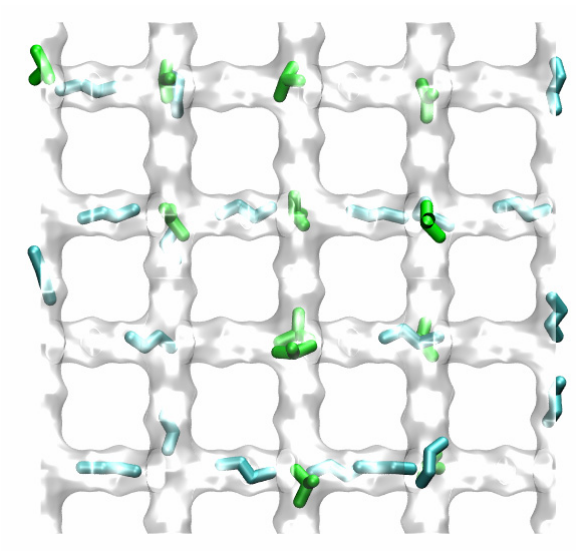

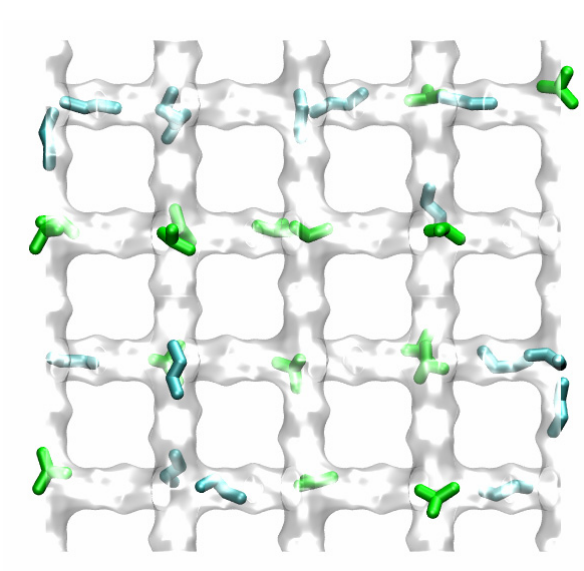

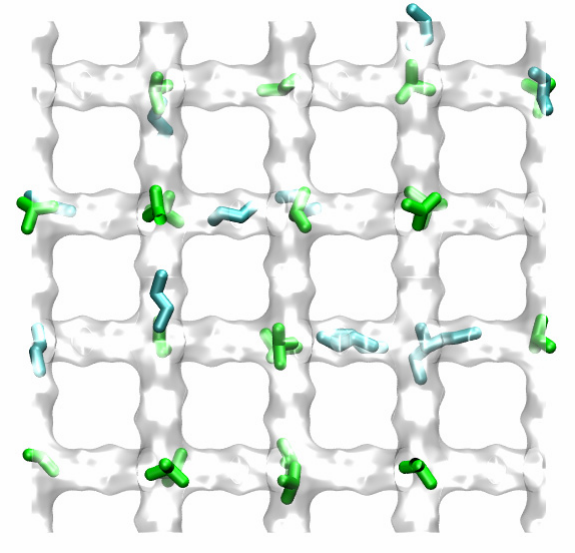

Snapshots showing location of nC4 - iC4 mixtures at in MFI at various loadings

the snapshots are 2 ucs deep

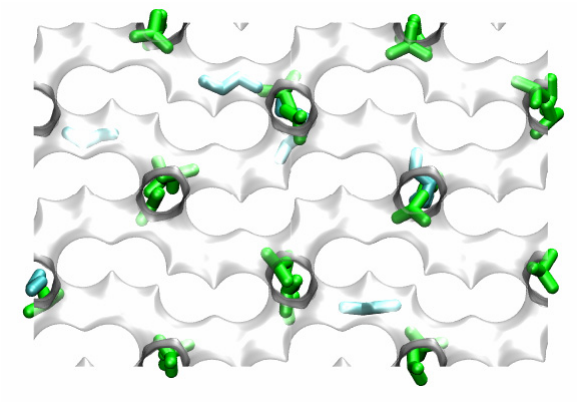

nC4 = 1 molecules/uc
iC4 = 3 molecules/uc

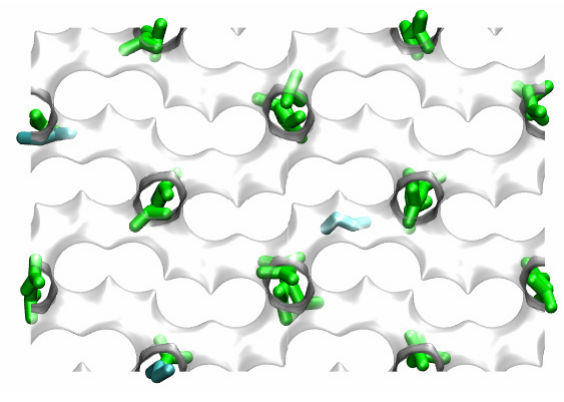

nC4 = 0.5 molecules/uc
iC4 = 3.5 molecules/uc

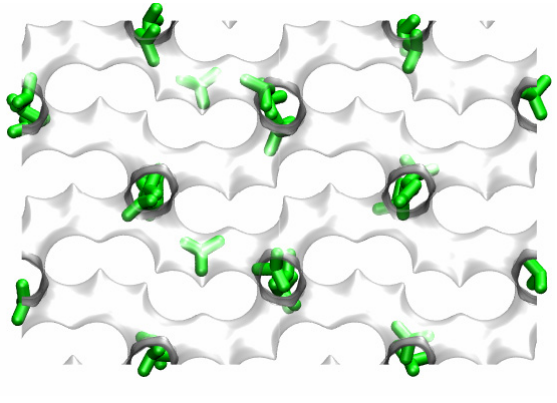

iC4 = 4 molecules/uc

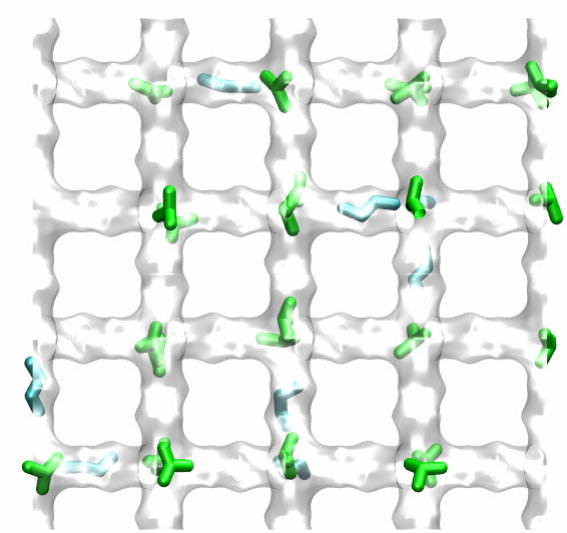

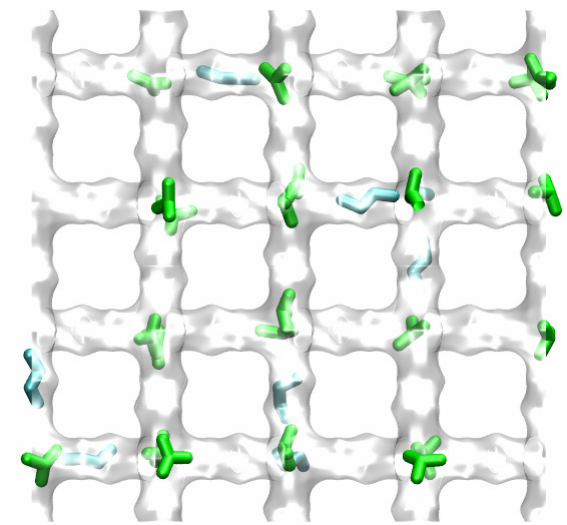

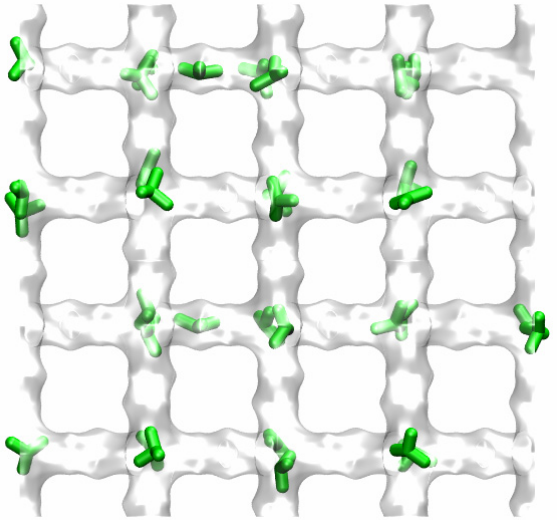

Snapshots showing location of nC4 - iC4 mixtures at in MFI at various loadings

the snapshots are 2 ucs deep

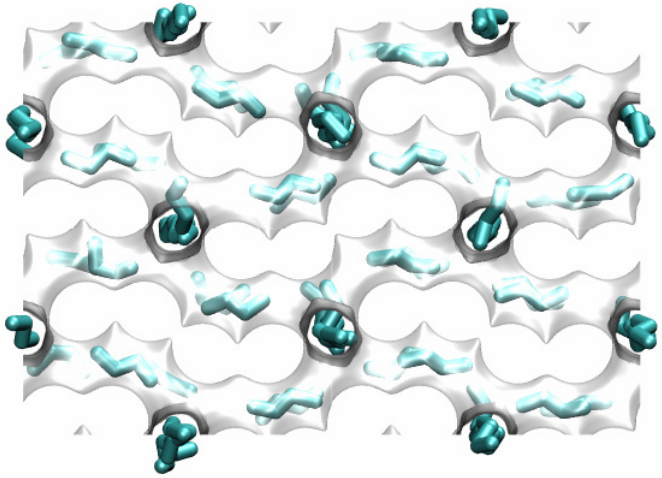

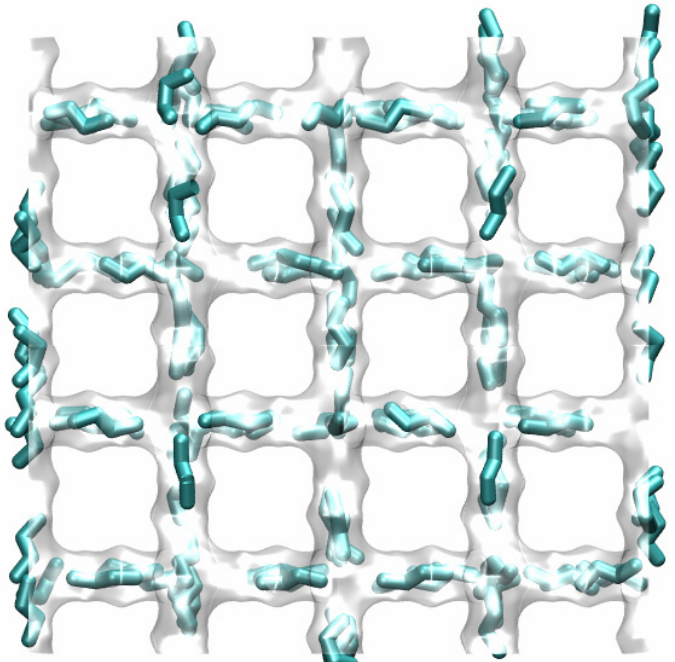

the snapshots are 2 ucs deep

MD simulations for pure nC4 diffusion in MFI

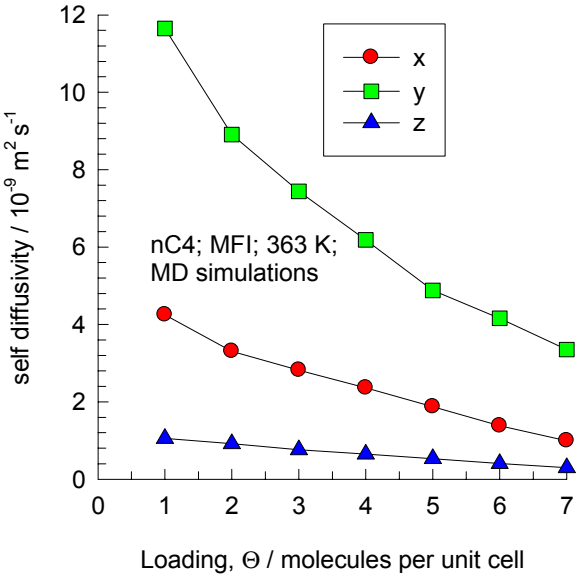

average self-diffusivity

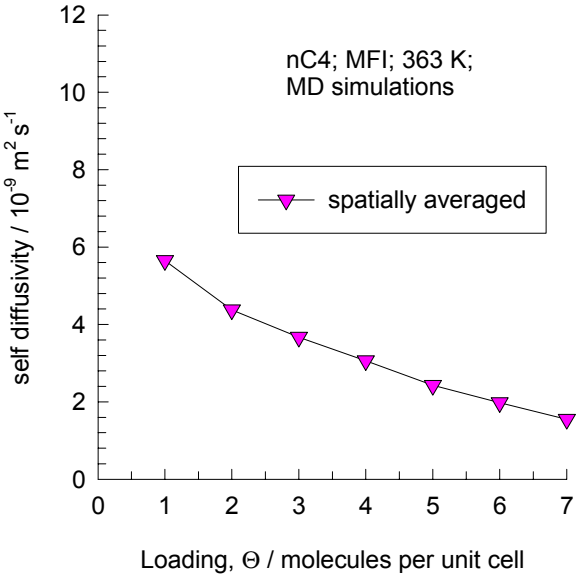

MD simulations for self diffusivity of nC4 in nC4-iC4 mixtures at total loading of 4 molecules per unit cell

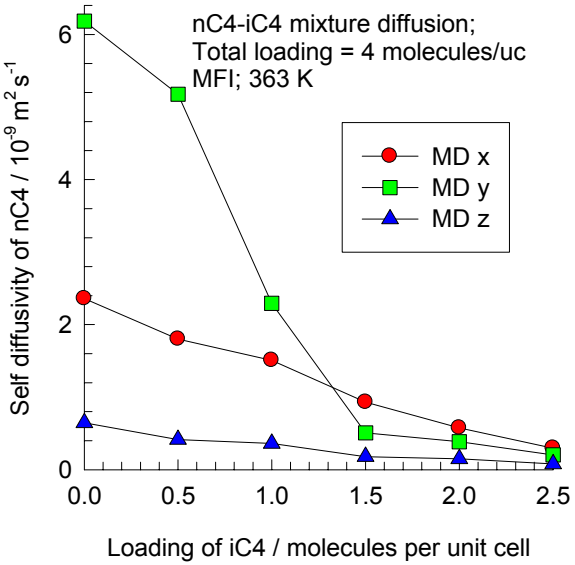

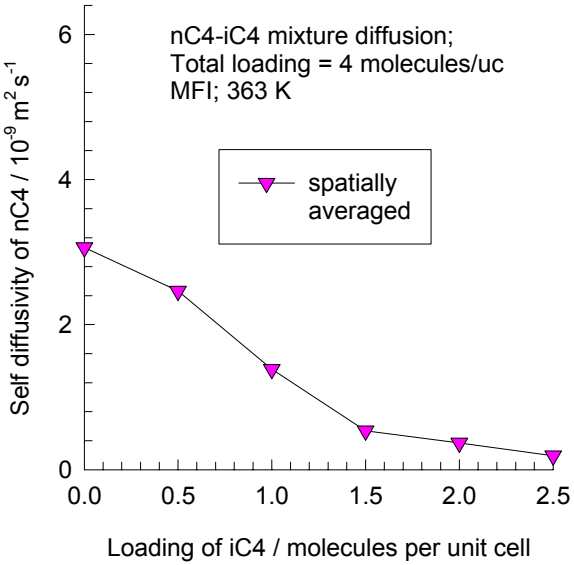

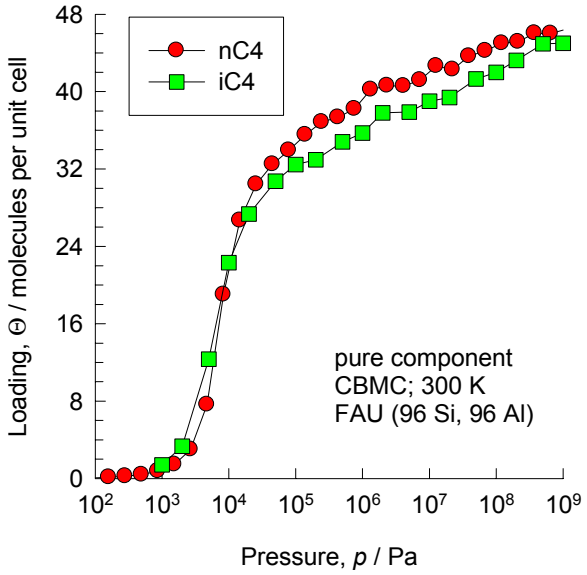

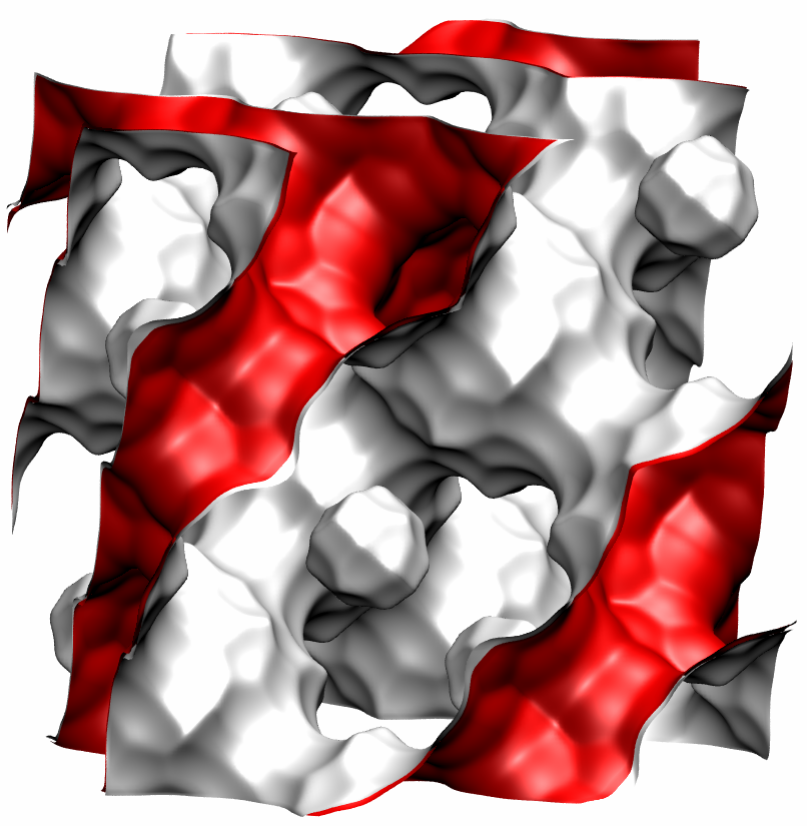

Pure component adsorption isotherms for nC4 and iC4 at 300 K in FAU (96 Si, 96 Al)

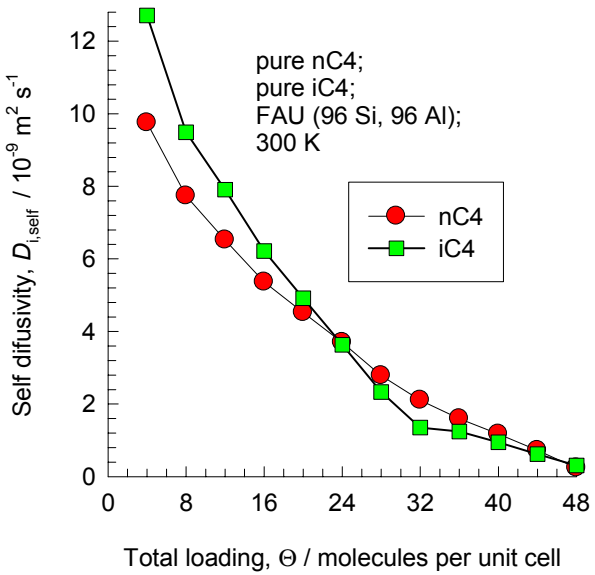

Pure component self diffusivities for nC4 and iC4 at 300 K in FAU

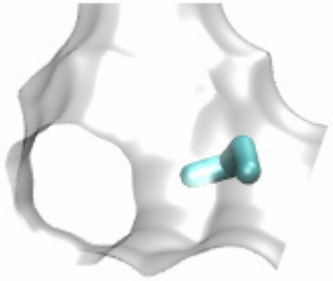

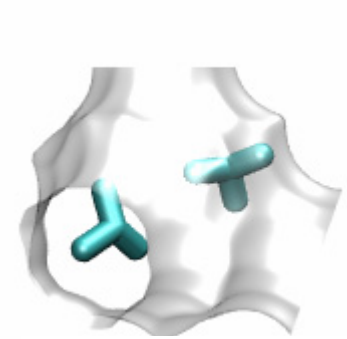

Self diffusivities in 50-50 mixtures of nC4 and iC4 at 300 K in FAU